Green Chemistry

Accepted Manuscript

This is an *Accepted Manuscript*, which has been through the Royal Society of Chemistry peer review process and has been accepted for publication.

Accepted Manuscripts are published online shortly after acceptance, before technical editing, formatting and proof reading. Using this free service, authors can make their results available to the community, in citable form, before we publish the edited article. We will replace this *Accepted Manuscript* with the edited and formatted *Advance Article* as soon as it is available.
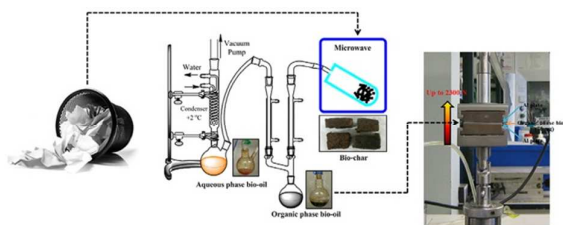
You can find more information about *Accepted Manuscripts* in the **Information for Authors**.

Please note that technical editing may introduce minor changes to the text and/or graphics, which may alter content. The journal's standard **Terms & Conditions** and the **Ethical guidelines** still apply. In no event shall the Royal Society of Chemistry be held responsible for any errors or omissions in this *Accepted Manuscript* or any consequences arising from the use of any information it contains.

The conversion of waste office paper (printed or photocopied) to bio-oil via low temperature (<200 ^{o}C) microwave-assisted pyrolysis, and its utilisation as an adhesive for aluminium-aluminium bonding, is reported. Application of the bio-oil (70 mg) to Al plates (50 mm x 50 mm) followed by curing at 160 ^{o}C for 8 h gave optimum tensile strength close to 2300 N.

Journal Name

ARTICLE

Low-temperature microwave-assisted pyrolysis of waste office paper and the application of bio-oil as an Al adhesive

Zhanrong Zhang[a], Duncan J. Macquarrie[a], Mario De bruyn[a], Vitaliy L. Budarin[a], Andrew J. Hunt[a], Mark J. Gronnow[b], Jiajun Fan[a], Peter S. Shuttleworth[c], James H. Clark[a] and Avtar S. Matharu*[a]

The conversion of waste office paper (printed or photocopied) to bio-oil via low temperature (<200 °C) microwave-assisted pyrolysis, and its utilisation as an adhesive for aluminium-aluminium bonding, is reported. The yield for the organic- and aqueous-phase bio-oil is 19% and 23%, respectively. The pyrolysis products were characterized by ICP-MS, ATR-IR, GC-MS and NMR to reveal broad categories of compounds indicative of sugars (carbohydrates), aromatics (phenolic in nature) and carbonyl-containing moieties. Application of organic phase bio-oil (70 mg) to Al plates (50 mm x 50 mm) followed by curing at different temperatures and time periods revealed maximum tensile strength of approximately 2300 N could be attained at 160 °C for 8 h cure. Also, at fixed temperature, the tensile strength increased with respect to increasing cure time. To achieve an in-depth understanding of the adhesive properties of bio-oil, a liquid – liquid fractionation of the organic phase bio-oil were conducted. The 'acidic' fraction showed far better adhesion properties than the 'neutral' fraction with no bonding achieved for the aqueous fraction. A combination of the 'acidic' and 'neutral' fraction gave better adhesion thus suggesting a possible synergistic or co-operative effect.

1. Introduction

Globally paper is one of the most widely recycled materials. For example, in 2011 the recycling rate in the EU was over 70%.[1] In theory, paper can be recycled up to six or seven times but in reality this is far from true. Paper cannot be recycled indefinitely as fibres get too short and worn to be useful in creating a new sheet of paper or cardboard box. The current average rate in Europe is 3.5; while world-wide the average is 2.4 times.[1] In an era of confidentiality and data protection, document shredding and/or milling of paper is on the rise which can render it ineffective for recycling as the resultant fibres become too short. Finely chopped or ground paper also causes maintenance problems and fire hazards when fed into certain types of paper mill machinery, and some mill machines simply cannot recognise small or shredded materials detrimental to paper quality.[2]

Thus, a significant amount of waste paper and board ends up in landfill or incineration, which is a loss of valuable cellulosic raw material and might have negative impacts on the environment. The recognition of the value of this reject material is now important, as the economic differential between price of paper for recycling and the cost of reject management is becoming marginal. Paper destined for recycling should be seen as a source for many valuable components to produce additional high value products alongside paper.[3]

The production of biofuels and other sugar derivatives (such as gluconic acid,[4] lactic acid,[5] etc.) from waste paper through biochemical conversion has been reported. Also, it has been estimated that the annual global production of bio-ethanol can be as much as 82.9 billion litres from waste paper, replacing 5.36% of petroleum consumption, with accompanying greenhouse gas (GHG) emissions savings of between 29.2% and 86.1%.[3] However, one disadvantage of biochemical conversion, which generally involves enzymatic hydrolysis, is the low enzymatic degradation rate of lignocellulosic materials due to the resistant crystalline structure of cellulose and the physical barrier formed by lignin that is associated with the cellulose.[6] Also, the high enzyme cost is another disadvantage for biochemical conversion from an economic point of view.[7]

Pyrolysis is considered to be a promising method for converting biomass into value-added products and aims to obtain char, gas and a liquid product (bio-oil) through thermal decomposition of biomass in the absence of oxygen. The pyrolysis process not only recovers the energy value of waste biomass, but also the

Green Chemistry

chemical value. There are several comprehensive reviews existing in the literature on pyrolysis of biomass/waste material for generation of value-added chemicals, fuels, materials and upgrading methods for pyrolysis products.[8-15] Bio-oil is potentially one of the most valuable products. It can be readily stored and transported, and can not only be used as a feedstock for the production of valuable chemicals, but also as a liquid fuel after upgrading.[8] Even though the recovery of pure chemical compounds from the complex bio-oil is technically feasible, it is unattractive economically due to its high costs and low concentrations of specific chemicals.[16] Also, although bio-oils have been tested successfully in engines, turbines and boilers, and have been upgraded to high-quality hydrocarbon fuels, its high energetic and financial cost is still presently unacceptable due to its high oxygen content and high viscosity and many other reasons.[8]

Recently, the combination of microwave with pyrolysis has attracted much attention due to the nature and many advantages of microwave heating, such as uniform and rapid internal heating of large biomass particles, instantaneous response for rapid start-up and shut down, energy efficiency, no need for agitation and controllability *etc*.[17] Also, microwave processing has now been widely accepted as an effective technique for both pilot scale and large continuous processing for waste treatment.[18] Luque *et al.* pointed out that microwave-assisted pyrolysis, especially at low temperatures, is a promising alternative for valorisation and processing of biomass and waste materials, and has potential to be integrated into future biorefineries.[19] In this context, Lam and Chase reviewed existing processes for converting waste to energy using microwave pyrolysis,[15] and Yin reviewed microwave-assisted pyrolysis of biomass for the production of biofuels.[20] In recent years, significant efforts have been devoted to the application of microwave pyrolysis to a vast array of biomass/waste materials, such as sewage sludge,[21-23] algae,[24-27] coffee hulls,[28] wheat straw,[29] cellulose,[30, 31] and other organic municipal solid wastes,[32-36] for valorisation. However, to our knowledge, there is no existing study on microwave-assisted pyrolysis of waste office paper to produce a bio-oil adhesive for Al - Al bonding.

Herein, we report our preliminary research on low temperature (<200 °C) microwave-assisted pyrolysis of milled waste office paper to yield bio-oil which may be used as a bio-based adhesive for metal-to-metal bonding. It is known that bio-oils can be used to generate adhesives.[37, 38] Indeed, several publications mentioned the use of the phenolic fraction of bio-oil, which derives mainly from the lignin, as a replacement for the phenol needed in the phenol / formaldehyde resin formulations, used to produce oriented strand board (OSR) and plywood.[39, 40] The milled waste office paper derived bio-oil was analysed and characterized using Fourier transform-infrared spectroscopy (FT-IR), Gas chromatography-mass spectroscopy (GC-MS), ^{13}C nuclear magnetic spectroscopy (^{13}C NMR) and inductively coupled plasma-mass spectrometry (ICP-MS). The adhesive properties of bio-oil were investigated by curing at various temperatures and time on Al plates. Also, an attempt was made to investigate the adhesive properties of bio-oil by liquid-liquid fractionation. The cured bio-oil polymers on the Al/bio-oil/Al interface was characterized with FT-IR and solid-state ^{13}C CP/MAS NMR with and without dipolar dephasing.

2. Experimental

2.1 Samples

Waste office papers (printed or photocopied) were obtained from the Green Chemistry Centre of Excellence, University of York and milled using a Farm Feed Solutions (UK) 12kW hammer mill with 5mm screen. The standard commercial samples and DMSO-d6 (>99% purity) for ^{13}C NMR analysis were purchased from Sigma Aldrich (UK) and used without further purification.

2.2 Low-temperature microwave-assisted pyrolysis

Low-temperature microwave-assisted pyrolysis of the milled waste office paper was conducted on a Milestone ROTO-SYNTH Rotative Microwave Reactor (Milestone Srl., Italy) fitted with a vacuum system. Thus, the condensable volatile compounds were collected as two phases (organic and aqueous) as shown in Figure 1. In the current work, the incondensable gas products were depleted from the system. Prior to microwave treatment at fixed power (1200 W, 2.45 GHz), milled office paper (150 g per run) was wet pressed into the microwave glass vessel and dried in oven at 105 °C for 48 h until a fixed weight was reached (moisture content less than 3% with a density of 0.3 g cm^{-3}). The process temperature was measured via an on-line infrared temperature probe and maintained below 200 °C, whilst the process pressure was monitored on the control panel throughout the process.
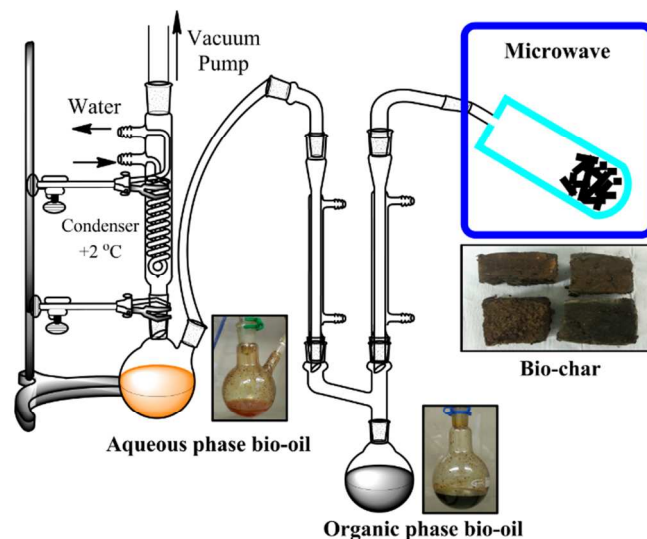

Fig. 1 Experimental set-up for microwave-assisted pyrolysis of milled waste office paper.

2.3 Characterization methods

Proximate analysis was conducted to determine the moisture, volatile matter, fixed carbon and ash content of milled waste office paper and bio-char using a Netzsch 409 Simultaneous Thermal Analyzer (STA). Detailed procedure was according to literature.[41] Ash content of bio-oils was determined as the residue material after heating bio-oil samples (100 mg) at 900 °C for 1 h in the Netzsch 409 STA. The temperature program was ramp from 30 °C to 900 °C at 50 °C min^{-1} and maintain at 900 °C for 1 h in an air atmosphere (100 ml min^{-1}).

Elemental analysis (C, H and N) was conducted on an Exeter Analytical CE440 Elemental Analyser. Sulfur contents of milled office paper and its MW-assisted pyrolysis products, together with total organic carbon (TOC) of aqueous phase bio-oil, were determined by Yara Analytical Services, York.

Calorific value (CV) of milled waste office paper and its pyrolysis products were determined using a Parr 6200 bomb calorimeter (Parr Instrument Company, Moline, IL, USA). CV measurements were carried out in triplicate and mean values were reported.

Water content of the organic phase bio-oil was determined on a GR Scientific Cou-Lo Aquamax Karl Fisher Titrator, using HYDRANAL®-Coulomat AK (anolyte solution) and HYDRANAL®-Coulomat CG-K (catholyte solution) as coulometric reagents, to avoid any interferences from ketones, amines or aldehydes.

The ATR-IR analysis of pyrolysis products (except the gas fraction) and scrapings of cured bio-oil polymers was performed on a Bruker Vertex 70 spectrometer in attenuated total reflectance (ATR) mode, with a resolution of 2 cm^{-1} and 64 scans.

The ^{13}C NMR characterization of bio-oils (both aqueous and organic phases) were performed on a Jeol ECX-400 NMR spectrometer at 100 MHz for 1024 scans, using the central resonance of DMSO-d6 (δC, 39.52 ppm) as the internal reference.

The GC-MS characterization of liquid products (bio-oils) was conducted on a Perkin Elmer Claus 500 gas chromatograph equipped with a Perkin Elmer Claus 560s mass spectrometer. The column was a non-polar ZB-5HT (30 m x 0.25 mm id x 0.25 μm film thickness) from Phenomenex (UK). The oven temperature programme was maintain at 60 ^{o}C for 1 min, then ramp 8 ^{o}C min^{-1} to 360 ^{o}C and hold for 1 min. The injection volume of sample is 1 μl. The identification of chromatographic peaks was by comparison with the NIST 2008 library.

Inductively coupled plasma-mass spectrometry (ICP-MS) of milled office paper and its MW-assisted pyrolysis products were conducted on an Agilent 7700x ICP-MS spectrometer to determine their metal contents. Prior to analysis, solid samples were acid digested in HCl and HNO$_3$ at a volume ratio of 3:1. Liquid samples (bio-oils) were diluted in acetone.

Solid-state ^{13}C CP/MAS NMR spectra were acquired using a 400 MHz Bruker Avance III HD spectrometer equipped with a Bruker 4mm H(F)/X/Y triple-resonance probe and 9.4T Ascend® superconducting magnet. The CP experiments employed a 1ms linearly-ramped contact pulse, spinning rates of 10000 ± 2 Hz, optimized recycle delays of 3 and 10 seconds (Al and glass, respectively), spinal-64 heteronuclear decoupling (at vrf=85 kHz) and are a sum of 1024 co-added transients. The dipolar dephasing experiments added a rotor-synchronized 180us dephasing delay with a pi refocussing pulse to minimize baseline distortion. Chemical shifts are reported with respect to TMS, and were referenced using adamantane (29.5 ppm) as an external secondary reference.

2.4 Liquid-liquid fractionation of bio-oil

The organic phase bio-oil (10 g) from low-temperature MW-assisted pyrolysis of office paper was dissolved in ethyl acetate at a 1:1 weight ratio and transferred to a separating funnel containing an equivolume of aqueous sodium hydroxide solution (2 M). After shaking and settling of the two layers, the aqueous layer was set aside whilst the organic layer was further extracted with aqueous 2M sodium hydroxide solution (5 x 100 mL). The organic layer was isolated, dried and the solvent removed *in vacuo* to give the 'neutral' fraction as a brown oil (1.9 g). The combined aqueous extract was acidified (1 M HCl), extracted with ethyl acetate (5 x 100 mL), dried (MgSO$_4$) and the solvent removed *in vacuo* to afford the 'acidic' fraction as a red-brown oil (2.5 g).

2.5 Curing experiments

Bio-oil (70 mg) was applied to two shot-blasted aluminium plates (50 mm x 50 mm) which were then pressed together using light pressure (finger-strength), weighted down with a stainless steel block (350 g) to mimic constant pressure and cured at various temperatures: 120 ^{o}C, 140 ^{o}C, 160 ^{o}C and 180 ^{o}C, for 4 and 8 h.

2.6 Mechanical strength tests

The tensile strength of the adhesive bond formed between the two aluminium plates post cure was measured using an Instron 3367 Dual Column System fitted with 3000 N capacity load cell, at a cross-head speed of 5 mm min^{-1}. The results reported were the averages of four measurements.

3. Results and discussion

3.1 Microwave assisted pyrolysis of milled office paper

The distribution of products as a result of low-temperature microwave-assisted pyrolysis of milled waste office paper is shown in Figure 2. This distribution is typical of waste biomass such as wheat straw.[29] The yield for the organic and aqueous phase bio-oils are 19% and 23%, respectively. This microwave-assisted pyrolysis process also yields a black char-like material with yield up to 43%. As the gas fraction was depleted from the microwave-assisted pyrolysis system by the vacuum pump, gas yield (15%) hence was calculated by difference.
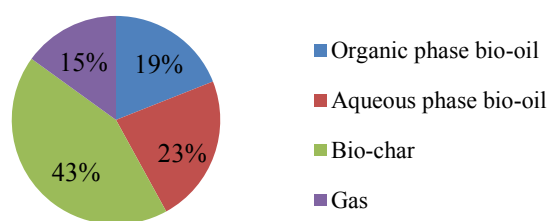

Fig. 2 Yield of low temperature microwave-assisted pyrolysis products.

The results for proximate and ultimate analysis and mineral elemental composition determined by ICP-MS, of the milled waste office paper and its low temperature MW-assisted

pyrolysis products are summarized in Table 1 and 2, respectively. As expected compared with original milled waste paper (13.6 MJ kg^{-1}) the resultant organic phase bio-oil has a higher calorific value (21.8 MJ kg^{-1}), *i.e.*, energy densified. The calorific value of the biochar (11.7 MJ kg^{-1}) is lower than the original waste paper raw (13.6 MJ kg^{-1}), which is due to its elevated content of inorganic matter, namely calcium carbonate ($CaCO_3$) and clays, commonly added during paper manufacturing,[42] The ICP-MS data (Table 2) shows very high levels of calcium in the biochar and the FT-ATR of the biochar (Figure 3D) shows prominent absorbance bands for calcium carbonate. In addition, the biochar has a high ash (inorganic content), as determined by TGA (33.8%), compared with that of milled office paper (12.8%). Also, significant amount of silica/silicon was present in both waste office paper as well as its MW-pyrolysis products. The high silica/silicon content most likely originates from kaolinite (aluminosilicate), water-soluble silica-based sizing agents and potential organosilane sizing agents that are added during paper manufacturing of high-quality coated paper.

Table 1 Proximate and ultimate analysis of milled waste office paper and its low-temperature MW-assisted pyrolysis products

	waste office paper	Organic phase bio-oil	Aqueous phase bio-oil	Bio-char
Proximate analysis (wt.%)				
Moisture	4.5	---	---	1.1
Volatile Matter	71.9	---	---	44
Fixed carbon	10.8	---	---	21.1
Ash	12.8	1.2	8.3	33.8
Ultimate analysis				
C^a	34.56	49.88	16.89	38.89
H^a	4.30	5.84	4.22	4.0
N^a	N.D.^{b}	N.D.	N.D.	N.D.
S^a	0.09	0.04	0.03	0.17
O$^{a, c}$	48.25	44.24	78.86	23.14
Heating Value (MJ kg^{-1})	13.6	21.8	---	11.7
TOC (mg l^{-1})^d	---	---	180,000	---
Water content (%)^e	---	2.6	---	---

^{a} wt%
^{b} N.D.: Not detected
^{c} Calculated by difference
^{d} TOC: Total organic carbon
^{e} Determined by Karl Fisher Titration

Table 2 Mineral contents of milled waste office paper and its low-temperature MW-assisted pyrolysis products

Element (ppm^a)	Milled office paper	Organic phase bio-oil	Aqueous phase bio-oil	Bio-char
Na	2463.83	194.33	123.36	3790.26
Mg	919.61	2.90	12.49	2414.23
Al	328.49	3.56	8.76	532.93
Si	27168.06	20668.25	23239.69	4956.24
K	1102.36	199.48	131.59	539.56
Ca	92877.53	712.27	411.83	243719.67
Cr	12.73	0.29	0.57	7.35
Mn	20.89	N.D.^{b}	N.D.^{b}	46.56
Fe	936.27	1.10	4.03	929.95
Cu	10.81	0.25	0.26	21.63
Zn	7.74	12.31	N.D.^{b}	13.86
As	4.64	6.01	2.51	11.32
Nb	0.45	0.04	0.52	0.05
Pd	0.31	0.02	0.11	0.63
Sn	1.13	18.84	1.69	16.53
Ir	0.16	0.03	0.05	0.04
Pt	0.05	0.03	0.05	0.06
Au	5.52	0.49	0.25	3.88
Pb	0.22	0.02	0.07	1.17

^{a} ppm refers to parts per million in mass
^{b} N.D.=Not Detected

3.2 ATR-IR analysis of pyrolysis products

The ATR-IR spectral analysis of the virgin milled office paper and subsequent pyrolysis products (except for gas) are shown in Figure 3. As can be seen in the spectrum of milled waste office paper (Figure 3A), the broad absorbance band between 3600 cm^{-1} and 3200 cm^{-1} is attributed to the O-H stretching vibration associated with cellulosic matter and sugars. Bands between 3000 cm^{-1} to 2800 cm^{-1} are originated by C-H stretching vibrations associated with saturated or aliphatic structures. A very weak but slightly broad absorption band centred 1630 cm^{-1} is due to the O-H deformation most likely from residual water or cellulosic matter. The very broad, strong band ranging from 1500 cm^{-1} to 1250 cm^{-1} is complex mixture of many absorbances: the C-H deformation (1370 cm^{-1}); the C-OH stretch (1315 cm^{-1}) and; the C-O-C stretch (1245 cm^{-1}), but is mainly due to $CaCO_3$ vibrations seen centred at 1415 cm^{-1}.[43] The C-O-C vibrations are further evidenced at 1160 cm^{-1} and 1100 cm^{-1}. The sharp band at 870 cm^{-1} also evidences the presence of $CaCO_3$, the content of which can be up to 8% in office paper.[42, 43] The band at 870 cm^{-1} may also correspond to torsional vibrations of methylene groups.[44]

A vast number of structural changes during the pyrolysis process can be seen from the spectra of the two fractions of bio-oil. From the spectrum of the organic phase bio-oil (Figure 3B), the most significant change with respect to milled waste office paper (Figure 3A) is the appearance of a medium intensity band centred at 1715 cm^{-1} corresponding to the C=O stretching vibration, indicating the presence of carbonyls. Also, the O-H stretching vibration drifts upward to higher wavenumber (3420 cm^{-1}) when compared with that of the raw material (3320 cm^{-1}), indicating a reduction in hydrogen bonding. The absorption band at 1623 cm^{-1} is due to the C=C stretching of alkene or aromatic compounds, but may also be associated with residual water. Figure 3C shows the IR spectrum of the aqueous phase bio-oil. The intense, broad O-H stretching vibration band between 3700 cm^{-1} and 3000 cm^{-1}, together with the intense carbonyl stretching vibration band (centred at 1715 cm^{-1}), suggest the presence of carboxylic acids. The band at 1640 cm^{-1} and the broad O-H stretching band confirm the presence of water. The aqueous phase bio-oil may also contain trace amounts of sugars and other compounds from the various bands in the region from 1500 cm^{-1} to 800 cm^{-1}.

bio-oils were broadly categorized to several groups according to chemical shifts, as summarized in Table 3.
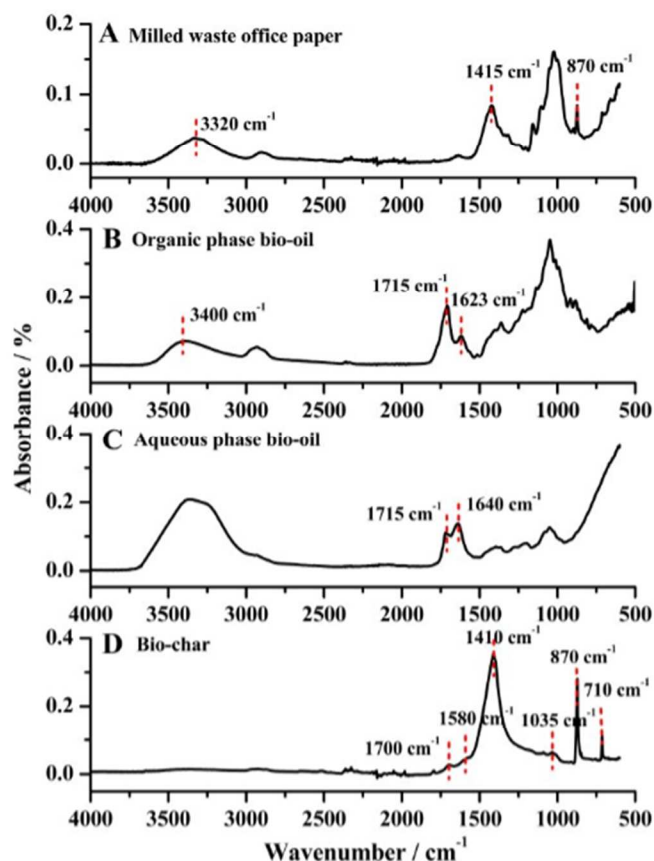

Fig. 3 ATR-IR spectra of (A) milled waste office paper (B) organic phase bio-oil (C) aqueous phase bio-oil (D) bio-char.

Compared with the spectrum of milled waste office paper, significant changes can be observed in the spectrum of bio-char (Figure 3D). The broad O-H stretching band between 3500 cm^{-1} and 3200 cm^{-1} has almost disappeared, indicating that the oxygen in the parent material was removed during the pyrolysis process and any acidic structures were cracked to leave a carbonaceous solid product. The intense band at 1410 cm^{-1} and the narrow band at 870 cm^{-1} and 710 cm^{-1} were assigned to $CaCO_3$. As carbon is formed during the pyrolysis process, once the char gets dark in colour, it acts as a black body and absorbs radiation over all frequencies, making most bands appear relatively weak. The presence of remaining organics is still evidenced by bands at 1700 cm^{-1}, 1580 cm^{-1} and 1035 cm^{-1}.

3.3 ^{13}C NMR characterization of bio-oils

In order to obtain more structural information, both the organic- and aqueous-phase bio-oils were investigated with ^{13}C NMR spectroscopy. Figure 4 shows the ^{13}C NMR spectra of the organic (Figure 4A) and aqueous phase bio-oil (Figure 4B). Due to the complex nature of bio-oil, the carbon assignments of
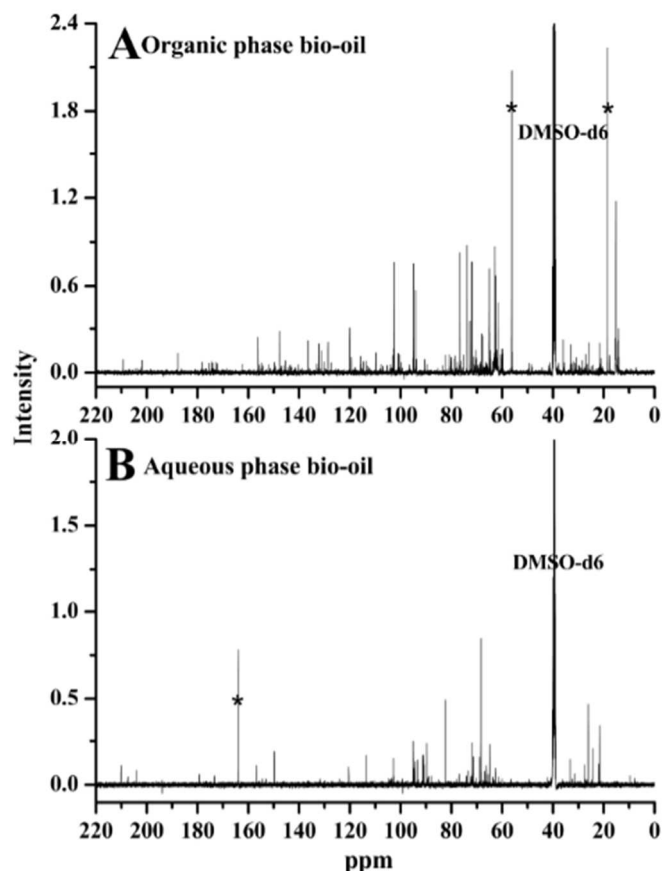

Fig. 4 ^{13}C NMR spectra of (A) organic phase bio-oil, (B) aqueous phase bio-oil. (All spectra used the central resonance of DMSO-d6 (δC, 39.52 ppm) as the internal reference).

∗ Possible artefacts

Table 3 Classification of bio-oil carbon contents according to chemical shift range

Chemical shift (ppm)	Carbon assignments
0 - 28	Short aliphatic structures
28 - 55	Long and branched aliphatic structures
55 – 105	Carbohydrate sugars, alcohols, ethers
110 - 165	Aromatics, olefins
165 - 180	Carboxylic acids, esters
180 - 220	Aldehydes, ketones

The spectrum of organic phase bio-oil shows more signals and of greater intensity than that of aqueous phase bio-oil between

55 – 110 ppm, suggesting more carbohydrates and its derivatives (e.g., levoglucosan, levoglucosenone) were trapped to the organic phase bio-oil.

A similar trend was observed in the aromatic region (110 – 165 ppm), which implies the organic phase bio-oil contains more aromatic compounds than the aqueous phase. Although the true identity has not been ascertained, possible compounds in this region could include 5-(hydroxymethyl)-2-furaldehyde (HMF) and phenolics. It is well documented in literature that simple phenols are present in bio-oils obtained from pyrolysis of cellulose and hemicellulose.[45, 46] These relatively small amounts of phenolics may either come from gas phase polymerization of small molecular weight unsaturated species[46] or from hydrothermolysis of HMF or other furan derivatives.[47] Luijkx *et al*. studied the reaction pathway for hydrothermal transition of HMF to 1,2,4–trihydroxybenzene, which may also present in the organic phase bio-oil.[47] A small portion of signals in this region may also attributed to phenolics derived from lignin pyrolysis, as lignin content in office paper is up to 6%, but this is yet to be fully ascertained.[42] The presence of (hetero-) aromatics is also evidenced by the ^{1}H NMR of organic phase bio-oil (see supplementary, Figure S1).

Both the organic and aqueous phase bio-oils contain carbonyl carbons: carboxylic acids and esters (165 – 180 ppm); ketones and aldehydes (180 – 215 ppm). The types of carbonyl carbons in the organic phase bio-oil are more various and complex than those of aqueous phase bio-oil. Among these, levulinic acid (4-oxopentanoic acid) is a common acid derived from HMF during pyrolysis of biomass. Signals between 0 – 55 ppm are attributed to aliphatic structures within the bio-oil.

The composition of pyrolysis products of milled waste office paper are similar to those obtained from pyrolysis of cellulose and hemicellulose. Some typical pyrolysis products, such as levoglucosan, levoglucosenone, HMF, and possibly 1,2,4–trihydroxybenzene were identified by comparison of the ^{13}C NMR chemical shifts of the organic phase bio-oil and commercial samples (see supplementary, Table S1).

3.4 GC-MS characterization of bio-oils

Gas chromatography - mass spectrometry (GC-MS) characterization was performed to identify the compounds obtained in the organic and aqueous phase bio-oil. Figure 5 shows the GC traces of organic (Figure 5A) and aqueous phase bio-oil (Figure 5B). Due to the complex composition of bio-oils, many peaks were detected for both phases; even though generally only 25% of bio-oil compounds can be observed by GC as most lignin and carbohydrate oligomers have insufficient volatility at the operating conditions of the instrument.[10, 48] As a result, complete separation of peaks is very difficult and only those separated products with considerable amounts were qualified. Table 4 and 5 shows the major identified compounds in the organic and aqueous phase bio-oil, respectively.

The main difference between the organic phase bio-oil and the aqueous phase is the absence of levoglucosan (peak marked '18' in Figure 5A) in the latter. The compounds identified in the organic phase bio-oil can be broadly categorized to several

groups: carbohydrates and their derivatives such as 1,4:3,6-dianhydro-πd-glucopyranose, 3,4-anhydro-d-galactosan and levoglucosan; possible phenolic compounds such as guaiacol, benzenetriol and 1,2-benzenediol (catechol) but their true identity is still to be ascertained; furanic structures such as furfural, tetrahydro-2,5-dimethoxyfuran and 5-(hydroxymethyl)-2-furaldehyde (HMF). The organic phase bio-oil also contains acetic acid and 4,4'-(1-methylethylidene)bisphenol (Bisphenol A) which is an additive in paper products.[49] The aqueous bio-oil (Figure 5B and Table 5) comprises a similar compositional profile in the range 3 - 10 mins albeit with fewer components. Water soluble acids are noted together with polar small molecules.
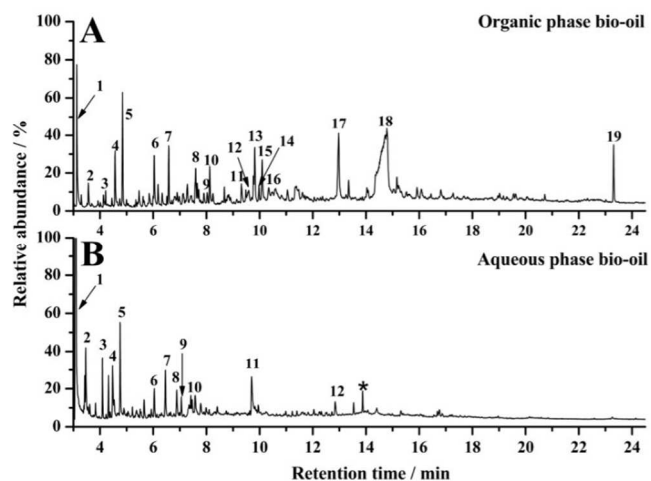

Fig. 5 GC-MS spectra of (A) organic and (B) aqueous phase bio-oils derived from MW-assisted pyrolysis of milled waste office paper
* Possible artefacts

Table 4 Major identified compounds in organic phase bio-oil[a]

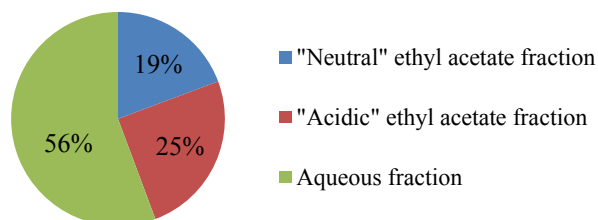| Peak Number	Retention time (min)	Identified Compound
1	3.13	Acetic acid
2	3.56	Furfural
3	4.15	Tetrahydro-2,5-dimethoxyfuran
4	4.57	2(5H)-Furanone
5	4.85	1,2-Cyclopentanedione
6	6.04	1-Hydroxy-2-pentanone
7	6.58	3-Methyl-1,2-cyclopentanedione
8	7.59	Guaiacol[b]
9	8.03	Levoglucosenone
10	8.12	Benzenetriol[b]
11	9.31	2-Furanmethanol
12	9.76	1,2-Benzenediol (Catechol)[b]
13	9.82	1,4:3,6-Dianhydro-πd-glucopyranose
14	10.09	3,4-Anhydro-d-galactosan
15	10.34	3-Methylbenzaldehyde
16	10.6	5-(hydroxymethyl)-2-furaldehyde (HMF)
17	12.96	5-Hydroxy-9-oxabicyclo[3.3.1]nonan-2-one
18	14.7	Levoglucosan
19	23.3	4,4'-(1-Methylethylidene)bisphenol

[a] According to NIST 2008 database.
[b] Tentative assignment

Table 5 Major identified compounds in aqueous phase bio-oil[a]

Peak Number	Retention time (min)	Identified Compound
1	3.13	Acetic acid
2	3.46	Furfural
3	4.09	Tetrahydro-2,5-dimethoxyfuran
4	4.49	2(5H)-Furanone
5	4.76	1,2-Cyclopentanedione
6	6.04	1-Hydroxy-2-pentanone
7	6.46	3-Methyl-1,2-cyclopentanedione,
8	6.88	1,2,3-Butanetriol
9	7.05	2,2-Dimethyl-acetoacetic acid ethyl ester
10	7.46	2,5-Dimethyl-4-hydroxy-3(2H)-furanone
11	9.69	1,4:3,6-Dianhydro-πd-glucopyranose
12	12.95	5-Hydroxy-9-oxabicyclo[3.3.1]nonan-2-one

[a] According to NIST 2008 database

3.5 Yield of fractionation of organic phase bio-oil

As the bio-oil is a complex mixture of sugar and its derivatives, (hetero-) aromatics, hydrocarbons and carbonyl compounds, to achieve some understanding of the bonding behaviour of bio-oil, the organic phase bio-oil (10 g) was subjected to liquid-liquid fractionation, from which three different bio-oil fractions (i. "neutral" ethyl acetate fraction, ii. "acidic" ethyl acetate fraction and, iii. aqueous fraction) were obtained. As shown in Figure 6, the yield for the "neutral" and "acidic" ethyl acetate fraction is 19% and 25%, respectively. For the aqueous fraction, as NaCl was generated during the acidification process, thus the yield for this fraction (56%) was calculated by difference.

Fig. 6 Yield of liquid-liquid separation of organic phase bio-oil.

3.6 13C NMR analysis of different bio-oil fractions

Figure 7 illustrates the 13C NMR spectra of "neutral", "acidic" ethyl acetate fraction and aqueous fraction bio-oil.
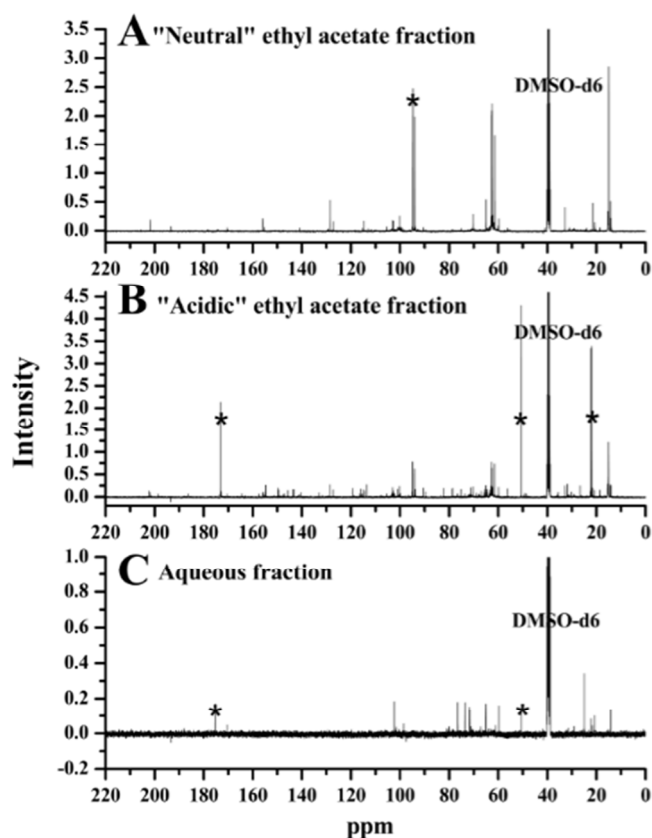

Fig. 7 13C NMR spectra of (A) "Neutral" ethyl acetate fraction (B) "Acidic" ethyl acetate fraction (C) Aqueous fraction bio-oil. (All spectra used the central resonance of DMSO-d6 (δC, 39.52 ppm) as the internal reference)
* Possible artefacts

Due to the complex chemical composition of the organic phase bio-oil, it is very hard to achieve complete separation. Basically, relatively a large percentage of (hetero-) aromatic compounds were separated in to the "acidic" ethyl acetate fraction, with many peaks detected in the (hetero-) aromatic portion of the spectrum of "acidic" ethyl acetate fraction bio-oil, ranging from 110 – 165 ppm. The sharp signals (centred at 94 ppm, 62 ppm and 15 ppm) shown in the spectrum of "neutral" ethyl acetate fraction bio-oil (Figure 7A) were also detected in the "acidic" ethyl acetate fraction bio-oil (Figure 7B), but with relatively smaller amounts within the "acidic" ethyl acetate fraction. These peaks are possibly due to ethers with relatively short carbon chains; this is further evidenced by a sharp signal at 15

ppm in the spectrum of "neutral" ethyl acetate fraction bio-oil. It is noteworthy that the spectrum of aqueous fraction bio-oil (Figure 7C) is almost 'clean' in the aromatic portion (105 – 165 ppm), with most peaks detected between 55 – 105 ppm (mostly carbohydrate sugars).

3.7 GC-MS characterization of different bio-oil fractions from liquid-liquid separation

Figure 8 shows the GC traces for the "neutral" (Figure 8A), "acidic" ethyl acetate fraction (Figure 8B) and aqueous fraction bio-oil (Figure 8C) resulted from liquid-liquid separation of the organic phase bio-oil.

It is noteworthy that compared with the GC trace of aqueous fraction bio-oil (Figure 8C), sugars were not detected in the two ethyl acetate fractions (Figure 8A and 8B), suggesting most carbohydrate sugars were remaining in the aqueous fraction. Most furans and acidic compounds were separated into the "acidic" ethyl acetate fraction; while some furans and acidic compounds were also detected in the "neutral" ethyl acetate fraction.
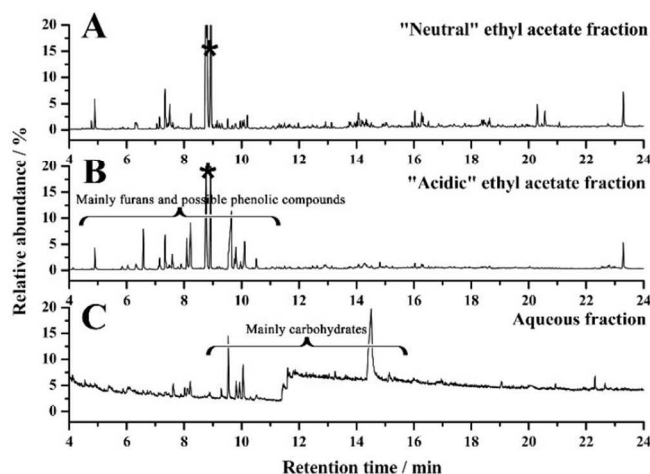

Fig. 8 GC-MS spectra of (A) "neutral", (B) "acidic" ethyl acetate fraction and (C) aqueous fraction bio-oil resulted from liquid-liquid separation of organic phase bio-oil
* Possible artefacts

3.8 Mechanical strength tests and bonding mechanism analysis

Figure 9 shows the average tensile strengths obtained with the organic phase bio-oil cured shot-blasted aluminium plates, oven cured at 120 ^{o}C, 140 ^{o}C, 160 ^{o}C and 180 ^{o}C for 4 and 8 h. In general, the bio-oil adhesive could bond the two Al plates with acceptable bond strengths at all curing temperatures and time periods. The maximum tensile strengths were obtained when cured at 140 ^{o}C and 160 ^{o}C, reaching around 2300 N (160 ^{o}C, 8 h). On the contrary, the minimum tensile strengths (around 900 N) were obtained when cured at 120 ^{o}C for 4 h. Also, the longer the curing time, the higher the Al-bio-oil-Al bond tensile strengths. This effect is more significant when cured at lower temperatures. For example, when cured at 120 ^{o}C, the tensile strength increased by ~50% to 1360 N (for 8 h cure) from around 900 N (for 4 h cure). However, at higher temperatures, the increase of tensile strengths was only around 15%.
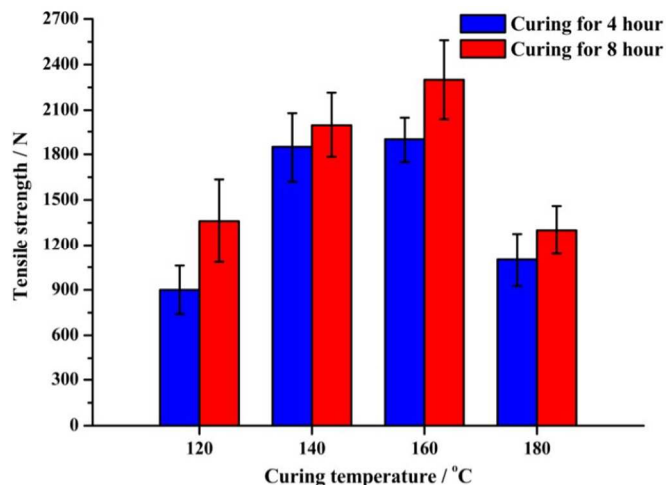

Fig. 9 Tensile strengths of organic phase bio-oil cured shot-blasted Al plates.

To get more structural information, the ATR-IR spectra of the organic phase bio-oil and scrapings from the organic/Al interface were compared (Figure 10). Many significant changes of functional groups occurred before and after curing of bio-oil. Compared with original organic phase bio-oil, the cured bio-oil polymer is characterized by a lower C=O:C=C ratio, suggesting polymerization occurred on carbonyl groups. Also, the C=C stretching frequency at 1617 cm^{-1} is characteristic for olefinic double bonds in five membered rings. The intensity of this peak increased after curing of the organic phase bio-oil on aluminium surfaces, suggesting the formation of conjugated / aromatic structures. This effect is also evidenced by a significant number of changes between 800 cm^{-1} and 900 cm^{-1}, which represents the C-H out of plane bending vibrations in substituted alkenes and aromatics. This may be caused by changes of the substitution patterns of such molecules during polymerization.

Another significant change is observed in the C-O stretching region (900 cm^{-1}-1200 cm^{-1}), the intensity of this band dramatically decreased, and many subtle changes occurred after curing. However, for bands centred at 1443 cm^{-1}, 1184 cm^{-1}, 1138 cm^{-1}, 1075 cm^{-1}, 1012 cm^{-1}, 918 cm^{-1}, 890 cm^{-1} and 856 cm^{-1}, they are either remaining or becoming more obvious in the spectra of scrapings. These bands are characteristic absorptions for levoglucosan, which is a common sugar derivative during pyrolysis of biomass. So it is possible that carbohydrate sugars were not significantly involved in the polymerization reactions during curing. This hypothesis is further investigated by following discussions.
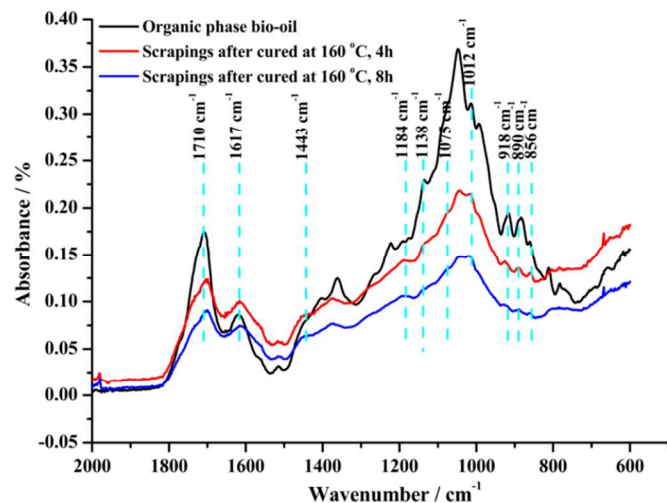
Fig. 10 ATR-IR spectra of organic phase bio-oil, scrapings of the Al – bio-oil – Al interface polymer formed at 160 °C for 4 and 8 h cure.

The scrapings from the bio-oil/Al interface (sample cured at 160 °C for 8 h, under which condition the maximum tensile strength was achieved) was further characterized with CP/MAS solid-state ^{13}C NMR. Also, a solid-state ^{13}C CP/MAS NMR with dipolar dephasing spectrum was recorded on this scraping to allow better assignment of resonance bands. In the latter case immobile carbons with directly attached hydrogens were significantly attenuated, so the spectrum will largely consist of the quaternary carbons and mobile carbons such as methyl groups. The spectra are shown in Figure 11 and overlapped with the liquid-state ^{13}C NMR of the organic phase bio-oil. From the ^{13}C CP/MAS NMR spectrum, the broad intense band between 50 ppm and 100 ppm is assigned to sugar carbons, which was almost not observed in the ^{13}C NMR spectrum with dipolar dephasing. The various resonance bands between 105 ppm and 165 ppm verify the presence of complicated aromatic structures. The resonance bands between 140 ppm and 160 ppm are attributed to quaternary aromatic carbons, which still exists in the dipolar dephasing ^{13}C spectrum. Bands between 105 ppm to around 140 ppm are aromatic carbons with one hydrogen atom attached, so the intensities of these bands decreased in the ^{13}C dipolar dephasing spectrum. The band between 100 ppm and 105 ppm in the ^{13}C NMR spectrum is characteristic resonance band for anomeric carbons in carbohydrate compounds. The scrapings also contain various carbonyl structures as proved by bands centered at 210 ppm and 175 ppm. In both cases the bands still remain in the spectrum of ^{13}C NMR with dipolar dephasing, suggesting they are mainly ketone (210 ppm) and ester (175) structures. Alkyl groups also present in the scrapings: methyl groups (0-20 ppm) and CH_2 structures (20 ppm - 50 ppm). The fact there is no significant change seen in the spectra of the post-cure scrapings is indicative of little of no decomposition of the main structural units, i.e., the aromatic and sugar moieties largely remain intact thus undergoing possible homo- and cross-coupling polymerisation reactions that help adhesion.
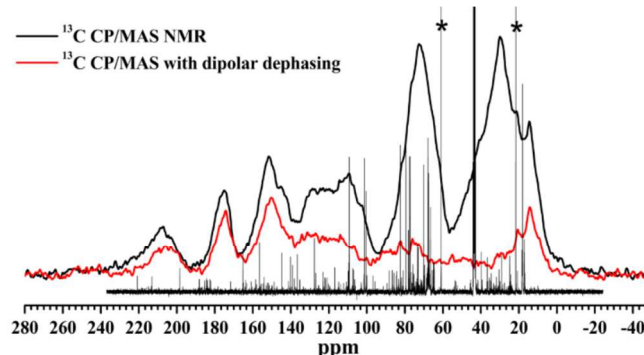

Fig. 11 Solid-state ^{13}C CP/MAS NMR spectrum of bio-oil/Al scraping (black) and ^{13}C CP/MAS NMR spectrum of bio-oil/Al scraping with dipolar dephasing (red), overlapped with liquid-state ^{13}C NMR of organic phase bio-oil
* Possible artefacts

The tensile strengths of the organic phase bio-oil, "neutral" and "acidic" ethyl acetate fraction bio-oil, the aqueous fraction solids, and the mixture of the two ethyl acetate fraction bio-oil cured Al plates are shown in Figure 12 (specimens cured with 70 mg bio-oil at 160 °C for 4 h). The tensile strengths obtained with different fractions bio-oil are all lower than that obtained with organic phase bio-oil. The tensile strength of the Al-"acidic" ethyl acetate fraction bio-oil-Al bond was about 1260 N, while the "neutral" ethyl acetate fraction could also bond the two Al plates but with very weak tensile strength (300 N). For the solids obtained from the aqueous fraction (water removed), they cannot bond the Al plates at all. As these solids are probably composed of carbohydrates mainly, it is obvious that the sugars by themselves could not bond substrates. An interesting observation is that when the "neutral" and "acidic" ethyl acetate fraction bio-oils were mixed by weight ratio of 1:1.25 (the same ratio as they present in bio-oil), the tensile strength of this mixture bonded Al plates (1460 N) were higher than those when bonded separately, but lower than that of organic phase bio-oil (1900 N). So it is possible that there is a *co-operative- or synergistic-effect* between the compounds from "neutral" and "acidic" ethyl acetate fraction and those from aqueous fraction that is responsible for the bonding properties of bio-oil, with the aromatic (mainly furanic) and acidic compounds mainly from "acidic" ethyl acetate fraction contributing more towards bonding. Bonding may be similar to phenol-formaldehyde cross-linking and this is being further investigated with a model compound study using catechol, HMF and levoglucosan, three components which have been tentatively identified in our pyrolysis products.
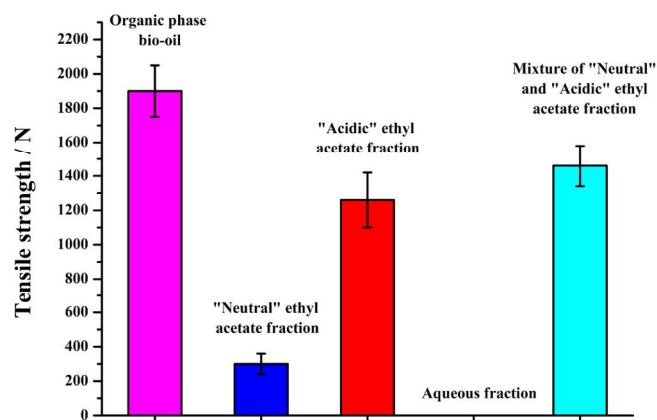
Fig. 12 Tensile strengths of organic phase bio-oil, "neutral" and "acidic" ethyl acetate and aqueous fraction bio-oil, and mixture of the "neutral" and "acidic" ethyl acetate fraction bio-oil cured Al plates (samples cured at 160 ^{o}C for 4 h).
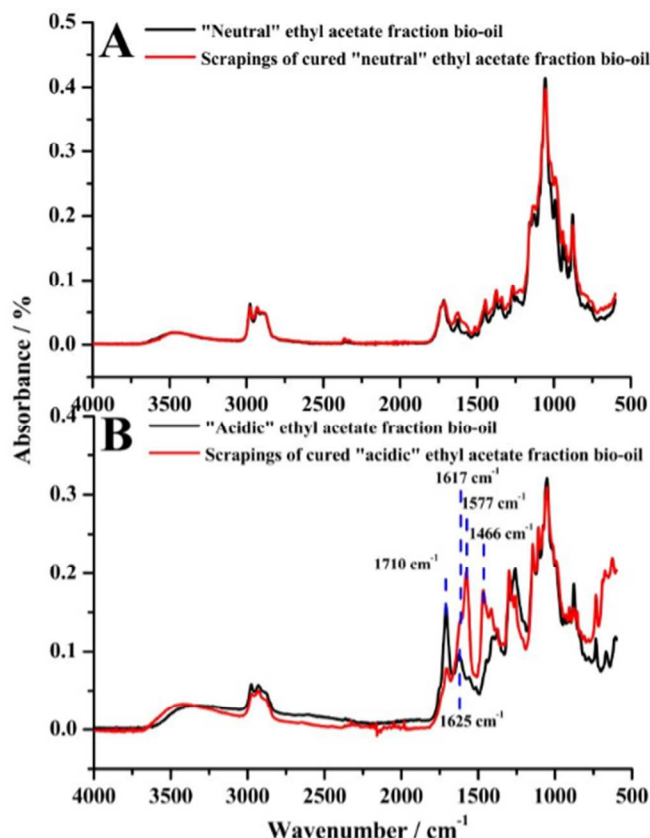

Fig. 13 ATR-IR spectra of (A) "neutral" ethyl acetate fraction bio-oil and scrapings of cured polymer of this fraction (B) "acidic" ethyl acetate fraction bio-oil and scrapings of cured polymer of this fraction (cured at 160 ^{o}C for 4 h).

This effect is further proved by comparing the ATR-IR spectra of the "neutral" and "acidic" ethyl acetate fraction bio-oil with the scrapings of formed polymers after curing (Figure 13). The polymer of the cured "neutral" ethyl acetate fraction bio-oil shows little structural changes (Figure 13A); while the polymer of cured "acidic" ethyl acetate fraction bio-oil shows dramatically significant changes after curing (Figure 13B).

Similar to the organic phase bio-oil, the intensity of the carbonyl peak at 1710 cm^{-1} decreased dramatically due to polymerization on the carbonyl bonds. The intensity of the C=C stretching vibration band increased dramatically and this stretching vibration band slightly shifts to lower wavenumber (1625 cm^{-1} to 1617 cm^{-1}). Also, significant structural changes and formation of new chemical bonds can be observed between 1630 cm^{-1} to 1450 cm^{-1} which is characteristic for skeletal vibrations of aromatic rings, suggesting the formation of new aromatic structures during curing. The formation of the significant shoulder peak between 1670 cm^{-1} to 1530 cm^{-1}, together with the dramatic intensity increase of the C=C stretching bond at 1617 cm^{-1}, probably implies the formation of conjugated aromatic structures during curing. This is also confirmed by the changes in the alkene/aromatic C-H out of plane bending region (800 cm^{-1} – 900 cm^{-1}). For the "acidic" ethyl acetate fraction bio-oil, after curing between Al plates, the O-H stretching drifts to higher wavenumber, and the C=O stretching peak at 1710 cm^{-1} slightly drifts to lower wavenumber, suggesting a reduction of hydrogen bonding occurred.

Conclusions

Waste office papers (printed or photocopied) were converted to bio-oil, bio-char and gas products via microwave-assisted low temperature (<200 ^{o}C) fast pyrolysis process. The total liquid yield is about 42%, with 19% for the organic phase and 23% for the aqueous phase bio-oil.

The potential application of organic phase bio-oil as adhesive for metal to metal bonding has been studied. Also, the effects of curing temperatures (120 ^{o}C, 140 ^{o}C, 160 ^{o}C and 180 ^{o}C) and curing time (4 and 8 h) have been investigated. A small amount of organic phase bio-oil (70 mg) could glue two aluminium plates with acceptable strengths (>900 N) at all these curing conditions. The highest tensile strengths around 2300 N were obtained when cured at 160 ^{o}C for 8 h. Also, the tensile strengths increase with curing time.

To achieve an in-depth understanding of the adhesive properties of bio-oil, a liquid-liquid fractionation of the organic phase bio-oil was conducted. Most (hetero-) aromatics were separated into the "acidic" ethyl acetate fraction, while the aqueous fraction mainly contains carbohydrate sugars. From the bonding experiments with different bio-oil fractions, it is revealed that there is a *co-operative- or synergistic- effect* most likely between phenolic and sugar derivatives within the bio-oil. However, the aromatic compounds are significant for good adhesion.

Acknowledgements

Notes and references

[a] Green Chemistry Centre of Excellence, Department of Chemistry, University of York. York, England. YO10 5DD.

[b] Biorenewables Development Centre, the Biocentre, York Science Park,

York, England. YO10 5NY.

c Departamento de Física de Polímeros, Elastómeros y Aplicaciones Energéticas, Instituto de Ciencia y Tecnología de Polímeros, CSIC, calle Juan de la Cierva, 3, 28006 Madrid, Spain.

1   European Recovered Paper Council, *Paper Recycling Monitoring Report 2012*.
     http://www.paperforrecycling.eu/uploads/Modules/Publications/WEB_lowres_Monitoring%20report%202012.pdf. Last accessed 17/07/2014.

2   H. Merrild, A. Damgaard and T. H. Christensen, *Resources, Conservation and Recycling*, 2008, **52**, 1391-1398.

3   A. Z. Shi, L. P. Koh and H. T. W. Tan, *GCB Bioenergy*, 2009, **1**, 317-320.

4   Y. Ikeda, E. Y. Park and N. Okuda, *Bioresource Technology*, 2006, **97**, 1030-1035.

5   E. Y. Park, P. N. Anh and N. Okuda, *Bioresource Technology*, 2004, **93**, 77-83.

6   G. Mtui and Y. Nakamura, *Biodegradation*, 2005, **16**, 493-499.

7   M. Alcalde, M. Ferrer, F. J. Plou and A. Ballesteros, *Trends in Biotechnology*, 2006, **24**, 281-287.

8   S. Czernik and A. V. Bridgwater, *Energy & Fuels*, 2004, **18**, 590-598.

9   A. V. Bridgwater, *Biomass and Bioenergy*, 2012, **38**, 68-94.

10   D. Mohan, C. U. Pittman and P. H. Steele, *Energy & Fuels*, 2006, **20**, 848-889.

11   A. V. Bridgwater and G. V. C. Peacocke, *Renewable and Sustainable Energy Reviews*, 2000, **4**, 1-73.

12   A. V. Bridgwater, D. Meier and D. Radlein, *Organic Geochemistry*, 1999, **30**, 1479-1493.

13   A. V. Bridgwater, *Chemical Engineering Journal*, 2003, **91**, 87-102.

14   M. Jahirul, M. Rasul, A. Chowdhury and N. Ashwath, *Energies*, 2012, **5**, 4952-5001.

15   S. S. Lam and H. A. Chase, *Energies*, 2012, **5**, 4209-4232.

16   M. F. Demirbas and M. Balat, *Energy Conversion and Management*, 2006, **47**, 2371-2381.

17   F. C. Borges, Z. Du, Q. Xie, J. O. Trierweiler, Y. Cheng, Y. Wan, Y. Liu, R. Zhu, X. Lin, P. Chen and R. Ruan, *Bioresource Technology*, 2014, **156**, 267-274.

18   D. E. Clark and W. H. Sutton, *Annual Review of Materials Science*, 1996, **26**, 299-331.

19   R. Luque, J. A. Menendez, A. Arenillas and J. Cot, *Energy & Environmental Science*, 2012, **5**, 5481-5488.

20   C. Yin, *Bioresource Technology*, 2012, **120**, 273-284.

21   J. A. Menéndez, M. Inguanzo and J. J. Pis, *Water Research*, 2002, **36**, 3261-3264.

22   A. Domínguez, J. A. Menéndez, M. Inguanzo and J. J. Pis, *Fuel Processing Technology*, 2005, **86**, 1007-1020.

23   A. Domínguez, J. A. Menéndez, M. Inguanzo, P. L. Bernad and J. J. Pis, *Journal of Chromatography A*, 2003, **1012**, 193-206.

24   N. Ferrera-Lorenzo, E. Fuente, J. M. Bermúdez, I. Suárez-Ruiz and B. Ruiz, *Bioresource Technology*, 2014, **151**, 199-206.

25   D. Beneroso, J. M. Bermúdez, A. Arenillas and J. A. Menéndez, *Bioresource Technology*, 2013, **144**, 240-246.

26   F. C. Borges, Q. Xie, M. Min, L. A. R. Muniz, M. Farenzena, J. O. Trierweiler, P. Chen and R. Ruan, *Bioresource Technology*, 2014, **166**, 518-526.

27   V. L. Budarin, Y. Zhao, M. J. Gronnow, P. S. Shuttleworth, S. W. Breeden, D. J. Macquarrie and J. H. Clark, *Green Chemistry*, 2011, **13**, 2330-2333

28   A. Domínguez, J. A. Menéndez, Y. Fernández, J. J. Pis, J. M. V. Nabais, P. J. M. Carrott and M. M. L. R. Carrott, *Journal of Analytical and Applied Pyrolysis*, 2007, **79**, 128-135.

29   V. L. Budarin, J. H. Clark, B. A. Lanigan, P. Shuttleworth, S. W. Breeden, A. J. Wilson, D. J. Macquarrie, K. Milkowski, J. Jones, T. Bridgeman and A. Ross, *Bioresource Technology*, 2009, **100**, 6064-6068.

30   V. L. Budarin, J. H. Clark, B. A. Lanigan, P. Shuttleworth and D. J. Macquarrie, *Bioresource Technology*, 2010, **101**, 3776-3779.

31   A. Al Shra'ah and R. Helleur, *Journal of Analytical and Applied Pyrolysis*, 2014, **105**, 91-99.

32   T. J. Appleton, R. I. Colder, S. W. Kingman, I. S. Lowndes and A. G. Read, *Applied Energy*, 2005, **81**, 85-113.

33   D. Beneroso, J. M. Bermúdez, A. Arenillas and J. A. Menéndez, *Fuel*, 2014, **132**, 20-26.

34   D. Beneroso, J. M. Bermúdez, A. Arenillas and J. A. Menéndez, *Journal of Analytical and Applied Pyrolysis*, 2014, **105**, 234-240.

35   A. Undri, L. Rosi, M. Frediani and P. Frediani, *Fuel*, 2014, **116**, 662-671.

36   S. S. Lam, A. D. Russell, C. L. Lee, S. K. Lam and H. A. Chase, *International Journal of Hydrogen Energy*, 2012, **37**, 5011-5021.

37   H. B. Goyal, D. Seal and R. C. Saxena, *Renewable and Sustainable Energy Reviews*, 2008, **12**, 504-517.

38   S. Xiu and A. Shahbazi, *Renewable and Sustainable Energy Reviews*, 2012, **16**, 4406-4414.

39   S. Tsiantzi and E. Athanassiadou, *PyNe Newsletter*, 2000, **10**, 10-11.

40   S. Cheng, Z. Yuan, M. Anderson, M. Leitch and C. Xu, *Journal of Applied Polymer Science*, 2012, **126**, E431-E441.

41   C. J. Donahue and E. A. Rais, *Journal of Chemical Education*, 2009, **86**, 222.

42   L. Wang, R. Templer and R. J. Murphy, *Applied Energy*, 2012, **99**, 23-31.

43   A. Méndez, J. M. Fidalgo, F. Guerrero and G. Gascó, *Journal of Analytical and Applied Pyrolysis*, 2009, **86**, 66-73.

44   A. M. Prima, R. G. Zhbankov and R. Marupov, *J Struct Chem*, 1965, **5**, 783-788.

45   S. D. Stefanidis, K. G. Kalogiannis, E. F. Iliopoulou, C. M. Michailof, P. A. Pilavachi and A. A. Lappas, *Journal of Analytical and Applied Pyrolysis*, 2014, **105**, 143-150.

46   R. J. Evans and T. A. Milne, *Energy & Fuels*, 1987, **1**, 123-137.

47   G. C. A. Luijkx, F. van Rantwijk and H. van Bekkum, *Carbohydrate Research*, 1993, **242**, 131-139.

48   C. A. Mullen, G. D. Strahan and A. A. Boateng, *Energy & Fuels*, 2009, **23**, 2707-2718.

49   C. Liao and K. Kannan, *Environmental Science & Technology*, 2011, **45**, 9372-9379.